Available online at www.sciencedirect.com
SCIENCE DIRECT®
Journal of Crystal Growth 265 (2004) 541–547
JOURNAL OF CRYSTAL GROWTH
www.elsevier.com/locate/jcrysgro

Fabrication of ZnCdSe quantum dots under Stranski–Krastanow mode

C.X. Shan[a,*], X.W. Fan[a], J.Y. Zhang[a], Z.Z. Zhang[a], X.H. Wang[a,b], Y.M. Lu[a], Y.C. Liu[a], D.Z. Shen[a], S.Z. Lu[a]

[a] *Key Laboratory of Excited State Processes, Changchun Institute of Optics, Fine Mechanics and Physics, Chinese Academy of Sciences, No.16 East South-Lake Road, Changchun 130033, PR China*

[b] *National Key Laboratory of High Power Semiconductor Laser, Changchun University of Science and Technology, No.7 Wei Xing Road, Changchun 130022, PR China*

Received 7 May 2003; accepted 5 February 2004
Communicated by R. James

Abstract

ZnCdSe quantum dot (QD) structures have been fabricated under the Stranski–Krastanow (S–K) mode on GaAs substrates by the metal-organic chemical vapor deposition (MOCVD) technique. Prior to the fabrication, the critical thickness of the ZnCdSe/GaAs structure, which plays a crucial role during the formation of the QD, was numerically calculated based on the theory of strain relaxation, and the QD was then prepared in terms of the calculated results. The formation of the QD was confirmed by atomic force microscopy (AFM) and photoluminescence (PL) measurements. By investigating the optical properties of the QD structures with different ZnCdSe thicknesses, the two-dimensional (2D) to 3D transition during the QD formation process was clearly observed, which confirms that the ZnCdSe QD was formed under S–K mode.
© 2004 Elsevier B.V. All rights reserved.

PACS: 68.65.+g; 78.55.Et; 07.79.Lh; 81.15.Gh

Keywords: A1. Low dimensional structures; A3. Metalorganic chemical vapor deposition; B1. Zinc compounds; B2. Semiconducting II–VI materials

1. Introduction

II–VI wide band gap semiconductors, especially ZnSe-based compounds, have been long studied for their potential applications to optoelectronic devices [1,2]. For example, laser diodes based on ZnCdSe have been successfully demonstrated to operate under a continuous-wave mode at room temperature [3]. Quantum dots, which have 3D confinement to electrons and holes, can produce higher quantum efficiency than 2D quantum wells and 1D quantum wires [4]. Therefore, the study of QD is of great current interest. Among several state-of-the-art preparation methods of QD, growth under the Stranski–Krastanow (S–K)

*Corresponding author. Fax: +86-431-4627031.
E-mail address: shancx2000@yahoo.com.cn (C.X. Shan).

0022-0248/$ - see front matter © 2004 Elsevier B.V. All rights reserved.
doi:10.1016/j.jcrysgro.2004.02.084

mode offers promise for the preparation of high-quality QD structures [5–7]. The basic idea of the S–K mode is to first deposit a thin film layer by layer, 3D islands then form on the 2D film when a certain critical thickness is reached. It is generally accepted that this growth mode needs a relatively large lattice mismatch between the epilayer and substrate, so most attention has been focused on III–V systems, particularly, InAs embedded in GaAs [8,9], which has a lattice mismatch of $\sim 7\%$. The reports on II–VI materials have been mainly focused on the CdSe/ZnSe system. In terms of the strain relationship, the CdSe/ZnSe system is identical to the InAs/GaAs system. However, with a room temperature band gap of 1.67 eV, the CdSe/ZnSe system can only cover the spectral range from red to green, and it is unable to operate in the blue and ultraviolet region. As is well known, $Zn_xCd_{1-x}Se$ can be used to extend its spectrum through the whole visible range by varying the x value. Therefore, the fabrication of ZnCdSe QDs is necessary for many optoelectronic applications. Additionally, the realization of laser diodes based on ZnCdSe with long-lifetime makes the study of ZnCdSe QD even more attractive. Zhang et al. have prepared ZnCdSe QD on ZnSe (1 1 0) by molecular-beam epitaxy (MBE) [10–12]. They grew a ZnSe layer under conditions that could not lead to layer-by-layer growth. This ZnSe layer inevitably resulted in a high degree of surface roughness. By depositing several monolayers of ZnCdSe, they obtained ZnCdSe QD. Therefore, their growth was not performed under the S–K mode.

In this paper, ZnCdSe QD was fabricated on GaAs substrate under the S–K mode by low-pressure MOCVD. The lattice mismatch between ZnCdSe and GaAs is smaller than the more commonly investigated CdSe/ZnSe system, and this relatively small mismatch will extend the 2D layer-by-layer growth region under the S–K mode. Thus, it is seemly for fabrication ZnCdSe QD by MOCVD technique, since it is difficult to control the thickness of the epilayer very precisely for this technique. In addition, the critical thickness, which is essential for the formation of QD under the S–K mode [13], is usually empirical in previous studies, which is adverse for accurate control of the size and density of the dots. In this study, the critical thickness was numerically calculated based on the strain relaxation model, and the growth was guided by the calculated results. Furthermore, to overcome the inconveniences caused by the absence of in-situ monitoring techniques, the PL measurements were performed on the ZnCdSe/ZnSe quantum structures with different ZnCdSe thicknesses, and more details of the formation process of the dots were revealed by the PL experiments.

2. Experiment

Samples were grown on GaAs (1 0 0) substrates by MOCVD equipment at 310°C with the growth pressure fixed at 24 mmHg. Dimethylzinc (DMZn), dimethylcadmium (DMCd), and hydrogen selenide (H_2Se) were used as precursors. The flow rates of the three precursors, which were controlled by three separate mass-flow-controllers, were kept at 1.6×10^{-6}, 4.3×10^{-7} and 5.5×10^{-6} mol/min, respectively. High-purity hydrogen was used as the carrier gas to transport the reactants into the reaction chamber. To avoid pre-reaction, the precursors were mixed just before reaching the substrate. The typical growth rates of the ZnCdSe and ZnSe layers were 0.6 and 0.7 Å/s. The topology of the QD samples was examined by a Digital Instrument nanoscope IIIa AFM system. These measurements were performed in air after the temperature of the growth chamber is cooled to room temperature, and the samples are removed from the growth chamber. PL measurements were carried out using a JY-630 micro-Raman spectrometer, and the 488-nm line of an Ar^+ laser was typically used as the excitation source if it is not otherwise stated.

3. Results and discussion

In the S–K growth mode, the islands are self-formed on a 2D wetting layer after a critical thickness is reached [14,15]. The critical thickness, according to People and Bean [16], can be

Table 1
Values of lattice constant and Poisson's ratio of ZnSe, CdSe and GaAs

	ZnSe	CdSe	$Zn_{0.56}Cd_{0.44}Se$	GaAs
Lattice constant a_0 (Å)	5.6676 [31]	6.05 [31]	5.8359	5.6531 [31]
Poisson's ratio v	0.38 [32]	0.492 [33]	0.429	

expressed by the following formula:

$$h_c \approx \left(\frac{1-v}{1+v}\right)\left(\frac{1}{16\pi\sqrt{2}}\right)\left[\frac{b^2}{a(x)}\right]\left[\frac{1}{f^2}\right]\ln\left(\frac{h_c}{b}\right), \quad (1)$$

where h_c denotes the critical thickness, b is Burger's vector, v is Poisson's ratio, and $a(x)$ is the bulk lattice constant of $Zn_xCd_{1-x}Se$ in our experiment. The lattice mismatch component, f, in the above formula is defined below [17]:

$$f = \frac{a_{ZnCdSe} - a_{GaAs}}{a_{GaAs}}, \quad (2)$$

where a_{ZnCdSe} and a_{GaAs} are the lattice constants of ZnCdSe and GaAs. Table 1 shows the lattice constants and Poisson's ratios of the compounds involved in this paper. Note that the values for $Zn_{0.56}Cd_{0.44}Se$ in our experiment are obtained by a linear interpolation between the corresponding values of ZnSe and CdSe. Using the lattice constants of $Zn_{0.56}Cd_{0.44}Se$ and GaAs in Eq. (2), one can obtain the lattice mismatch value for f to be 0.032. It should be noted that this value is much smaller than the 7% lattice mismatch for more commonly studied systems. The Burger's vector of b is usually taken as 4.008 Å [17]. Eq. (1) can then be rewritten as follows after taking all the relevant parameters into account:

$$h_c = 15.1255 \ln\left(\frac{h_c}{4.008}\right). \quad (3)$$

Defining variable ζ as

$$\zeta = \frac{h_c}{15.1255} \quad (4)$$

one can plot Eqs. (3) and (4) in one graph, as shown in Fig. 1. The intersection of the two lines indicates the critical thickness of the $Zn_{0.56}Cd_{0.44}Se$/GaAs system. The critical thickness of this system is about 3.1 nm as indicated by the dotted line in Fig. 1. It is obvious that the thickness is significantly larger than that of

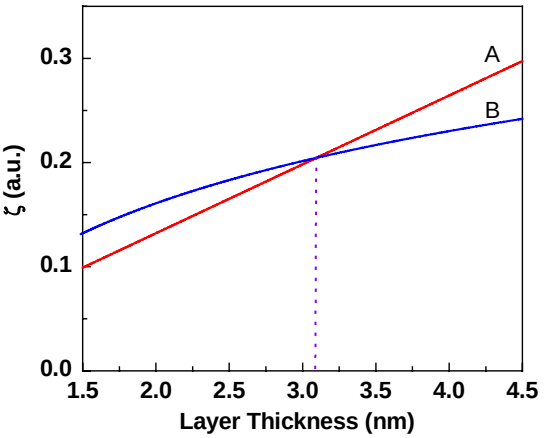

Fig. 1. Plot of the critical thickness of $Zn0_{.56}Cd_{0.44}Se$/GaAs system. Here line A denotes $\zeta = h_c/15.1255$, while line B is the representation of $\zeta = \ln(h_c/4.008)$. The abscissa of intersection yields the value of the critical thickness.

CdSe/ZnSe system, which is estimated empirically to be ~3 monolayers. This thicker critical thickness will extend the 2D layer-by-layer stage during the formation of QD, and it is advantageous for operating in an MOCVD system due to the difficulty in precisely controlling the epilayer thickness.

The QD was prepared under the guidance of the above-depicted calculation. The QD used for AFM measurements was deposited directly onto a GaAs substrate without any buffer layer. The QD samples for PL measurements were fabricated in the following way: the GaAs wafer was first covered by a 170-nm ZnSe buffer layer followed by a 5-period ZnCdSe/ZnSe deposition. The thicknesses of the ZnCdSe and ZnSe layers in this experiment were 3 and 14 nm, respectively. Subsequently, a 42-nm ZnSe layer was used to cap the structure.

The AFM image taken after deposition of a $Zn_{0.56}Cd_{0.44}Se$ layer with 3.0-nm thickness onto a

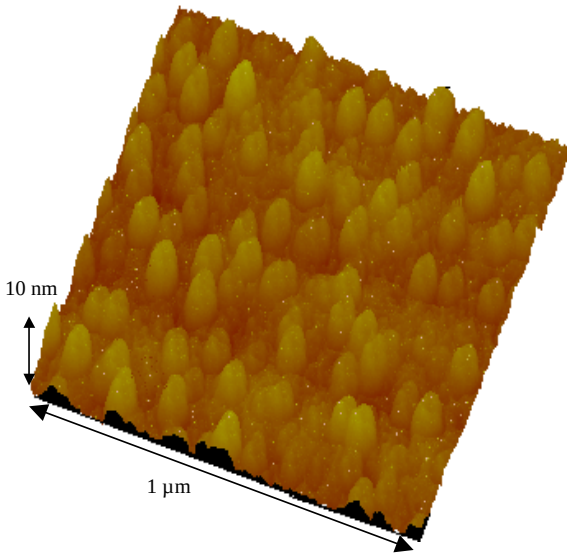

Fig. 2. AFM topology of ZnCdSe QD on GaAs substrates.

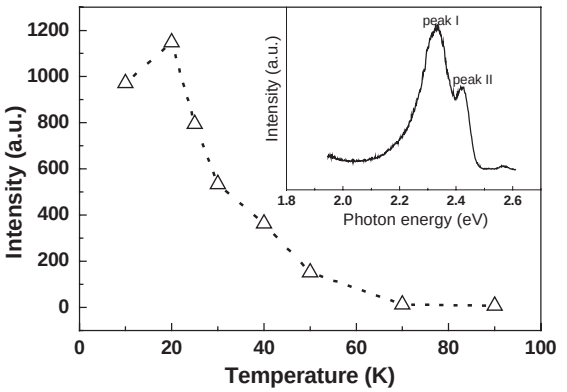

Fig. 3. Temperature dependence of the PL integrated-intensity of a typical ZnCdSe QD sample. The inset shows a representative PL spectrum of the QD sample at 10 K.

GaAs substrate is shown in Fig. 2. As can be seen from the figure, there appear to be some dome-shaped islands on the substrate. The average base diameter and height of the islands are $\sim$60 and 7 nm, and the density is about $8 \times 10^9\,\mathrm{cm}^{-2}$.

The temperature dependence of the PL intensity of a typical ZnSe-buried QD sample is shown in Fig. 3, in which a dotted line is used to connect the data points. This PL measurement was performed in a variable temperature cryostat in the temperature range of 10–90 K under the excitation of the 337.1-nm line of an NRG-90 N_2 laser. The signals were collected by a R955 photomultiplier tube. The inset of Fig. 3 shows the PL spectrum of the investigated sample at 10 K, Two emission peaks appear in the spectrum, and they are labeled as peak I and peak II. Given the positions and full-width-at-half-maximum data of the two peaks, peak I is attributed to the emission from the 3D dot layer, while peak II is thought to be the emission from the 2D wetting layer. The most prominent feature in the temperature-dependent luminescent intensity of the QD sample is that the intensity increases with temperature below 20 K and decreases rapidly as the temperature increases above 20 K. This observation agrees with that observed for CdSe [6,18–20] and CdTe [21] QD systems, and it can be recognized as a fingerprint of the QD luminescence [21].

Since the formation process of QD is a fast process, the MBE equipment employed to the preparation of QD structures is usually equipped with a reflection high-energy electron diffraction (RHEED), which can reveal the transition in growth mode in the initial stage of QD formation. However, RHEED cannot be applied to MOCVD technique for low vacuum level in this technique. Therefore, researchers usually remove the QD sample from the growth chamber when the temperature is cooled to about room temperature, then the QD sample was investigated by ex-situ AFM [22,23]. This cooling process will take about 1 h. Thus, the initial formation stage of the QD cannot be studied in this way. Furthermore, after being taken out of the growth chamber, the QD sample will be exposed to air, which may change the component of the sample due to the oxidation process [24,25]. Yang et al. introduced a slow surface diffusion process to equalize the cooling stage of the QD sample, and in this way, they observed the formation of QD by AFM [26]. This method overcomes the first inconvenience mentioned above, but is helpless to the second shortcoming of AFM measurement. Some groups equipped their MOCVD with in-situ AFM equipment [27]. However, equipment process is not only complicated but also costly. In the following

paragraph, in terms of the idea that the different formation stages of QD have different PL characters, we investigate the formation process of ZnCdSe QD by PL measurements. The PL measurements, on one hand, can cover the initial formation stage of QD; on the other hand, the dot was taken out of the growth chamber for PL measurements after they are covered by ZnSe cap layer, which insures that the QD is not affected by the air.

In our experiment, a series of samples with different $Zn_{0.56}Cd_{0.44}Se$ thicknesses were prepared according to the growth procedure of the above-mentioned ZnSe-buried structures. Note that after ZnCdSe was deposited, a 60-s interruption was introduced for the forming and ripening of the QD. Fig. 4 shows the PL spectra of the series of samples. The ZnCdSe thickness in samples A, B, C, D and E are 1.8, 2.1, 2.5, 3.0 and 3.6 nm, respectively, and the PL intensities are all normalized in intensity for simplicity. The PL spectra of samples A and B show an approximately Gaussian line-shape, sample C shows an asymmetry one, and samples D and E show clearly two emission peaks. The peaks on the low-energy side for samples C, D and E are labeled as peak I, and those on the high-energy side are labeled as peak II. As indicated above, 3D dots form on the 2D wetting layer when a certain critical thickness is reached. The ZnCdSe thicknesses for samples A and B are well below the above-calculated critical thickness of about 3.1 nm. Therefore, the emission peaks for samples A and B come from the 2D ZnCdSe layer, which indicates that the QD in our experiment progresses initially in a 2D mode. By increasing the ZnCdSe thickness from 1.8 to 2.1 nm, the emission peak shows a clear redshift, and this shift is due to the elimination of the quantum confinement effect in the ZnCdSe/ZnSe quantum structure. The asymmetric PL line-shape for sample C can be well fitted by two Gaussian lines, as indicated by the dotted lines in the figure. We believe that the two lines are related to 3D dot and 2D wetting layer for the following reasons: According to our previous result, surface diffusion plays an important role during the formation of the QD [28]. The 2.5 nm layer is below the critical thickness, and the surface diffusion, which is a slow process compared to the formation process of QD, can lead to significant fluctuations on the ZnCdSe surface. As a result, some areas reach or exceed the critical thickness, and the QD begins to form there within the 60-s growth interruption. Therefore, peak I in sample C is thought to originate from the 3D dot, while peak II is attributed to the 2D wetting layer. It is noticeable that the emission from the 2D wetting layer has almost the same width as that from the 3D dot layer, which may result from either the poor layer-by-layer characteristics of our samples or the surface fluctuations caused by mass transfer during the formation of the dots. The assignment is supported by sample D, in which the ZnCdSe layer is almost equal to the calculated critical thickness. Two distinct peaks appear in sample D. Peak I is on the low energy side of that for sample C, while peak II is on the high energy side of the counterpart for sample C. Furthermore, the intensity ratio of peak I to peak II is enhanced for sample D. The above-mentioned observations can be well understood based on the formation process. Once the 3D dots appear, significant mass transfer from the 2D wetting layer to the QD occurs [29,30]; consequently, the size of the 3D dots increases at the cost of the 2D wetting layer. Therefore, the emission peak of 3D dot redshifts, while that of the 2D wetting layer shifts to the high energy side due to the attenuation of the wetting

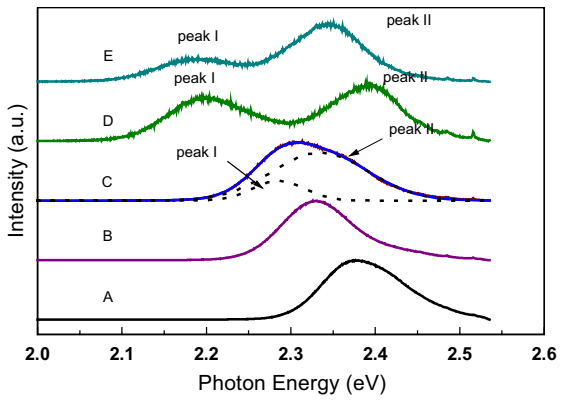

Fig. 4. PL spectra of ZnCdSe/ZnSe quantum structure with different ZnCdSe thicknesses at room temperature. The ZnCdSe thicknesses are (a) 1.8 nm, (b) 2.1 nm, (c) 2.5 nm, (d) 3.0 nm, (e) 3.6 nm.

layer. This may also be the reason for the slight blueshift of peak II for sample C compared to the emission peak for Sample B. As for the relative variation in emission intensity of peak I and peak II for the different samples, it is due to the change in quantity of the 2D wetting layer and the 3D dot layer resulted from the mass transfer. The appearance of a distinct emission peak from the 3D dots for sample D verifies with the validity of the calculated critical thickness. When the ZnCdSe thickness is increased further, for instance, to 3.6 nm, peak I shows slight redshift, while peak II redshifts drastically in comparison with that for sample D. By comparing the emission peak of the QD for sample D with that for sample E, one can deduce that the increase in dot size is very small when the additional 0.6 nm of ZnCdSe was delivered, and most of the excrescent ZnCdSe materials is used to increase the thickness of the wetting layer. As a result, the emission peak from the 2D wetting layer redshifts drastically, while that from the 3D dot layer show negligible redshift. In addition, the intensity ratio of peak I to peak II for sample E decreases as compared to that for sample D.

According to the above depictions, the dot formation process, which was usually studied by AFM in previous literatures, was investigated in detail by PL measurements.

4. Conclusions

In conclusion, we have prepared ZnCdSe QD on GaAs substrates under the S–K mode by low-pressure MOCVD. The critical thickness was numerically calculated using a strain relaxation model. AFM images and the appearance of an inflection point in the temperature-dependent PL intensity demonstrate the formation of QD in our samples. Optical studies of the formation process of the QD reveal that the growth progresses layer-by-layer initially, and then there is a significant mass transfer from the 2D layer to 3D dot once the critical thickness is reached. This confirms that the formation of the QD in our experiment is under the S–K mode. The formation of ZnCdSe QD on GaAs opens a way for preparing QD on substrates with relatively small mismatch under the S–K mode.

Acknowledgements

This research is financially supported by the Major Project of the National Natural Science Foundation of China (60336020), the "863" Advanced Technology Research Program (2001AA31112), the National Natural Science Foundation of China (60278031, 60176003, 60376009), and the Knowledge Innovation Program of CIOMP.

References

[1] X.W. Fan, J. Woods, IEEE Trans. ED 28 (1981) 428.
[2] M. Klude, D. Hommel, Appl. Phys. Lett. 79 (2001) 2523.
[3] M.A. Haase, P.F. Baude, M.S. Hafedon, J. Qiu, J.M. Depuydt, H. Cheng, S. Guha, G.E. Hofler, B.J. Wu, Appl. Phys. Lett. 63 (1993) 2315.
[4] Y. Arakawa, H. Sakaki, Appl. Phys. Lett. 40 (1982) 939.
[5] F. Heinrichsdorff, A. Krost, M. Grundmann, D. Bimberg, F. Bertram, J. Christen, A. Kosogov, P. Werner, J. Crystal Growth 170 (1997) 568.
[6] S.H. Xin, P.D. Wang, A. Yin, C. Kim, M. Dobrowolska, J.L. Merz, J.K. Furdyna, Appl. Phys. Lett. 69 (1996) 3884.
[7] R. Nötzel, J. Temmyo, T. Tamamura, Nature 369 (1994) 131.
[8] G. Wang, S. Fafard, D. Leonard, J.E. Bowers, J.L. Merz, P.M. Petroff, Appl. Phys. Lett. 64 (1994) 2815.
[9] C. Heyn, D. Endler, K. Zhang, W. Hansen, J. Crystal Growth 210 (2000) 421.
[10] B.P. Zhang, T. Yasuda, Y. Segawa, H. Yaguchi, K. Onabe, E. Edamatsu, T. Itoh, Appl. Phys. Lett. 70 (1997) 2413.
[11] B.P. Zhang, W.X. Wang, T. Yasuda, Y. Segawa, K. Edamatsu, T. Itoh, Appl. Phys. Lett. 71 (1997) 3370.
[12] B.P. Zhang, W.X. Wang, T. Yasuda, Y. Segawa, K. Edamatsu, T. Itoh, J. Crystal Growth 184/185 (1998) 237.
[13] D. Leonard, K. Pond, P.M. Petroff, Phys. Rev. B 50 (1994) 11687.
[14] M. Kitamura, M. Nishioka, R. Schur, Y. Arakawa, J. Crystal Growth 170 (1997) 563.
[15] M. Geiger, A. Bauknecht, F. Adler, H. Schweizer, F. Scholz, J. Crystal Growth 170 (1997) 558.
[16] R. People, J.C. Bean, Appl. Phys. Lett. 47 (1985) 322.
[17] K. Pinardi, U. Jain, S.C. Jain, H.E. Maes, R. Van Overstraeten, M. Willander, J. Appl. Phys 83 (1997) 4724.
[18] J.L. Merz, S. Lee, J.K. Furdyna, J. Crystal Growth 184/185 (1998) 228.

[19] Y. Murase, T. Ota, N. Yasui, A. Shikimi, T. Noma, K. Maehashi, H. Nakashima, J. Crystal Growth 214/215 (2000) 770.
[20] K. Maehashi, N. Yasui, Y. Murase, T. Ota, T. Noma, H. Nakashima, J. Electron. Mater. 29 (2000) 542.
[21] G. Karczewski, S. Mackowski, M. Kutrowski, T. Wojtowicz, J. Kossut, Appl. Phys. Lett. 74 (1999) 3011.
[22] Z.H. Ma, I.K. Sou, K.S. Wong, Z. Yang, G.K.L. Wong, J. Crystal Growth 201/202 (1999) 1218.
[23] I. Suemune, T. Tawara, T. Saitoh, K. Uesugi, Appl. Phys. Lett. 71 (1997) 3886.
[24] J.B. Smathers, E. Kneedler, B.R. Bennett, B.T. Jonker, Appl. Phys. Lett. 72 (1998) 1238.
[25] M. Grün, F. Funfrock, P. Schunk, Th. Schirmmel, M. Hetterich, C. Klingshirn, Appl. Phys. Lett. 73 (1998) 1343.
[26] Yi. Yang, D.Z. Shen, J.Y. Zhang, X.W. Fan, Z.H. Zhen, X.W. Zhao, D.X. Zhao, Y.N. Liu, J. Crystal Growth 220 (2000) 286.
[27] P.R. Kratzert, M. Rabe, F. Henneberger, Appl. Surf. Sci. 166 (2000) 332.
[28] Y. Yang, D.Z. Shen, J.Y. Zhang, X.W. Fan, Z.H. Zhen, X.W. Zhao, D.X. Zhao, J. Crystal Growth 225 (2001) 431.
[29] T.R. Ramachandran, R. Heitz, P. Chen, A. Madhukar, Appl. Phys. Lett. 70 (1997) 640.
[30] Y. Yang, D.Z. Shen, J.Y. Zhang, X.W. Fan, B.S. Li, Y.M. Lu, Y.C. Liu, Y.N. Liu, J. Crystal Growth 233 (2001) 785.
[31] B.L. Sharma, R.K. Purohit, Semiconductor Heterojunctions, Pergamon Press, New York, 1974, p. 24.
[32] C.F. Cline, H.L. Dunegan, G.W. Henderson, J. Appl. Phys. 38 (1967) 1944.
[33] T. Yokogawa, M. Ogura, T. Kajiwara, J. Appl. Phys. 62 (1987) 2843.